Conformation-Directing Effects of a Single Intramolecular Amide-Amide Hydrogen Bond: Variable-Temperature NMR and IR Studies on a Homologous Diamide Series

Samuel H. Gellman,* Gregory P. Dado, Gui-Bai Liang, and Bruce R. Adams

Contribution from the S. M. McElvain Laboratory of Organic Chemistry, Department of Chemistry, University of Wisconsin, 1101 University Avenue, Madison, Wisconsin 53706.
Received June 25, 1990

Abstract: We have studied intramolecular hydrogen bonding in a homologous series of diamides (compounds **1-6**) in methylene chloride, 9:1 carbon tetrachloride/benzene, and acetonitrile. By correlating variable-temperature ^{1}H NMR and IR measurements, we have shown that the temperature dependence of the amide proton NMR chemical shift ($\Delta\delta/\Delta T$) can provide qualitative (and in some cases quantitative) information on the thermodynamic relationship between the intramolecularly hydrogen bonded and non-hydrogen-bonded states of flexible molecules. Among the hydrogen-bonded ring sizes represented in the diamide series, the intramolecular interaction is particularly enthalpically favorable in the nine-membered hydrogen-bonded ring (compound **4**). Variable-temperature IR and NMR data indicate that the internally hydrogen bonded state of diamide **4** is 1.4-1.6 kcal/mol more favorable enthalpically than the non-hydrogen-bonded state, in methylene chloride solution; the non-hydrogen-bonded state is 6.8-8.3 eu more favorable entropically in this solvent. In contrast, there appear to be much smaller enthalpy differences between the internally hydrogen bonded and non-hydrogen-bonded states of diamides **2** and **3**. Our findings are important methodologically because the temperature dependences of amide proton chemical shifts are commonly used to elucidate peptide conformation in solution. Our results show that previous "rules" for the interpretation of such data are incomplete. In non-hydrogen-bonding solvents, small amide proton $\Delta\delta/\Delta T$ values have been taken to mean that the proton is either entirely free of hydrogen bonding or completely locked in an intramolecular hydrogen bond over the temperature range studied. We demonstrate that an amide proton can be equilibrating between intramolecularly hydrogen bonded and non-hydrogen-bonded states and still manifest a small chemical shift temperature dependence (implying that the hydrogen-bonded and non-hydrogen-bonded states are of similar enthalpy).

Introduction

Proteins are inherently flexible molecules, but usually they must adopt compact and highly ordered conformations to perform their biological functions.[1] Many globular proteins fold spontaneously to their native structures in aqueous solution.[1,2] How does the sequence of covalent bonds in the protein molecule specify the biopolymer's three-dimensional folding pattern? In the most general terms, the answer to this question has been accepted for some time: tertiary protein structure results from noncovalent interactions among different sites on the peptide chain and between the peptide chain and its environment. (This "environment" can be aqueous solution, the nonpolar interior of a lipid bilayer, the surface of a biomembrane, or the surface of another biopolymer, among other things.) Unfortunately, more detailed answers to this question are not presently available. It is impossible to predict a protein's folding pattern from its amino acid sequence on the basis of the fundamental principles of noncovalent interactions.[3] What limited success there has been in the prediction of three-dimensional protein structure derives from empirical correlations with the locations of individual amino acid residues in known structures.[3] Prediction methods based on such correlations have some practical utility, but they do not necessarily provide insight on the origins of protein structural stability.

Two factors contribute to the difficulty of deducing the origins of protein secondary and tertiary structural stability: (1) each of the many noncovalent interactions that occur in a folded protein makes only a small contribution to the overall thermodynamic difference between folded and unfolded states; (2) the constituent interactions cannot be considered separately, because they may compete with or reinforce one another.[4] A central issue in understanding protein conformation is discerning how molecular folding patterns result from the energetic balance that must be achieved as many noncovalent contacts tend toward their individual optimum configurations.

We are studying the forces that determine protein structure by examining how the balance among a modest number of noncovalent interactions influences the solution conformations of small molecules.[5,6] The work we describe here focuses on the conformation-directing effects of a single intramolecular amide-amide hydrogen bond, which we have begun to explore by monitoring the equilibrium between intramolecularly hydrogen bonded and non-hydrogen-bonded states of diamides **1-6**. These studies shed

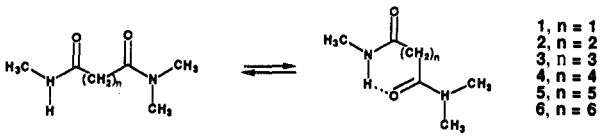

light on the competition between the enthalpic drive for internal hydrogen bond formation and the forces that oppose hydrogen-bonded ring closure. The difference in molecular complexity between these diamides and proteins is large, but it will be impossible to understand biopolymer architecture at the most fundamental level until the dynamic behavior of appropriate model systems is elucidated.

The structural simplicity of diamides **1-6** allows us to evaluate spectroscopic methodology for detection and thermodynamic assessment of internal hydrogen bonding in solution. In particular, comparison of IR and ^{1}H NMR data for the amide proton is straightforward with these compounds. Equilibration between hydrogen-bonded and non-hydrogen-bonded states for a given

(1) Creighton, T. E. *Proteins: Structures and Molecular Principles*; Freeman: New York, 1984.

(2) It has recently become clear that at least some protein-folding processes in vivo are orchestrated or modulated by other proteins; see: Ellis, J. R.; Heminingsen, S. M. *Trends Biochem. Sci.* **1989**, *14*, 339, and references cited therein.

(3) Fasman, G. D. In *Prediction of Protein Structure and the Principles of Protein Conformation*; Fasman, G. D., Ed.; Plenum Press: New York, 1989; pp 193-316.

(4) (a) Alber, T. In *Prediction of Protein Structure and the Principles of Protein Conformation*; Fasman, G. D., Ed.; Plenum Press: New York, 1989, pp 161-192. (b) Finney, J. L.; Gellatly, G. J.; Golton, I. C.; Goodfellow, J. *Biophys. J.* **1980**, *32*, 17.

(5) For a preliminary report on this work, see: Gellman, S. H.; Adams, B. R. *Tetrahedron Lett.* **1989**, *30*, 3381.

(6) (a) Gellman, S. H.; Adams, B. R.; Dado, G. P. *J. Am. Chem. Soc.* **1990**, *112*, 460. (b) Dado, G. P.; Desper, J. M.; Gellman, S. H. *J. Am. Chem. Soc.* **1990**, *112*, 8630.

0002-7863/91/1513-1164$02.50/0

amide proton is almost always fast on the NMR time scale, and observed amide proton chemical shifts are weighted averages of the chemical shifts of contributing states. IR spectroscopy is, in principle, more useful for detecting amide hydrogen bonding equilibria, because the much shorter time scale of IR measurements permits observation of distinct N–H stretch absorptions for equilibrating hydrogen-bonded and non-hydrogen-bonded states.[7] The application of IR spectroscopy to complex molecules (e.g., peptides) is limited, however, by signal overlap when more than one or two amide NH groups are present.[8]

The temperature dependence of the amide proton NMR chemical shift ($\Delta\delta/\Delta T$) has been widely used as a tool for studying intramolecular hydrogen bonding in peptides.[9,10] The initial systems examined in this way were conformationally rigid cyclic peptides dissolved in strongly hydrogen bonding solvents.[11] In such cases, each amide proton is either locked in a transannular hydrogen bond or engaged in intermolecular hydrogen bonding with the solvent. Small $\Delta\delta/\Delta T$ values in these systems can be reasonably interpreted to indicate an internally hydrogen bonded NH, while large $\Delta\delta/\Delta T$ values suggest a solvent-exposed NH. More recently, $\Delta\delta/\Delta T$ data have been obtained for *flexible* peptides, in both hydrogen-bonding and non-hydrogen-bonding solvents,[9,10] but the interpretation of such data from these conformationally mobile systems is less straightforward than for the rigid cyclic peptides.

Our work represents the first attempt to establish the significance of amide proton $\Delta\delta/\Delta T$ data for flexible molecules by correlating those data with variable-temperature IR measurements. Because diamides **1–6** can experience only one internal hydrogen bond each, the equilibration between non-hydrogen-bonded and internally hydrogen bonded states can be fully characterized by IR. The IR data can then be used as an independent check on the interpretation of the ^{1}H NMR $\Delta\delta/\Delta T$ data in terms of a two-state model. As will be discussed below, our results reveal that $\Delta\delta/\Delta T$ data can provide quantitative thermodynamic information on intramolecular hydrogen bonding and that the qualitative "rules" for interpretation of amide proton NMR $\Delta\delta/\Delta T$ data obtained in non-hydrogen-bonding solvents are more complex than has been previously recognized.

Results

Infrared Spectroscopy.[7,12] At room temperature, no intermolecular amide–amide hydrogen bonding is detectable in a 1 mM *N*-methylacetamide solution in CH_2Cl_2. The only absorption observed in the N–H stretch region under these conditions occurs at 3460 cm^{-1} (a broader band at 3320 cm^{-1}, for intermolecularly hydrogen bonded N–H, grows in at higher amide concentrations). Venkatachalapathi et al. have reported that the non-hydrogen-bonded N–H stretch absorption for *N*-methylacetamide occurs at 3490 cm^{-1} in the gas phase;[13] the 30-cm^{-1} shift observed in CH_2Cl_2 solution presumably results from a weak interaction of the amide proton with a solvent chlorine atom. We shall refer to these solvent-associated N–H stretch absorptions as indicative of a "non-hydrogen-bonded" state below, to distinguish them qualitatively from IR absorptions arising from amide–amide hydrogen-bonded states.

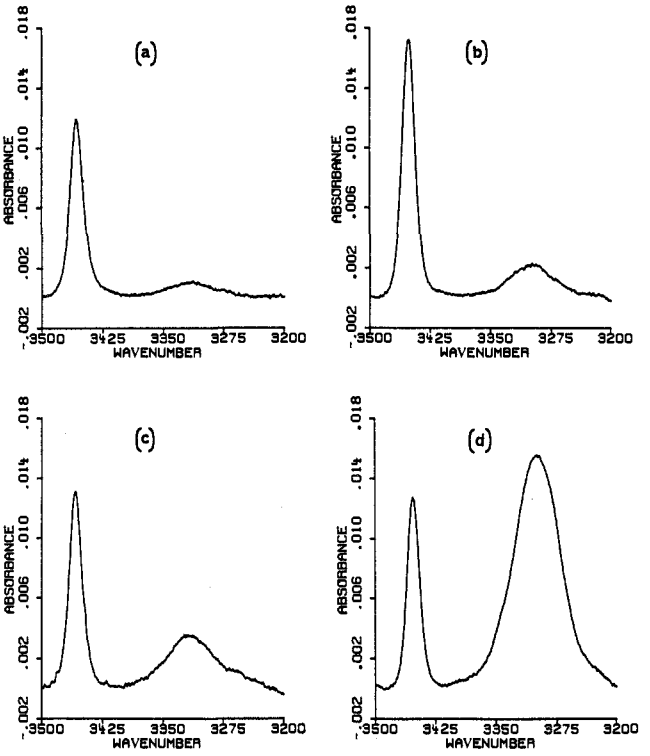

Figure 1. N–H stretch region FT-IR spectral data for 1 mM diamide solutions in CH_2Cl_2. (a) Diamide **3** at 297 K. (b) Diamide **3** at 186 K. (c) Diamide **4** at 297 K. (d) Diamide **4** at 186 K. In each case, the spectrum of pure CH_2Cl_2, at the appropriate temperature, has been subtracted from the diamide spectrum. The sharp bands at 3450–3460 cm^{-1} are assigned to non-hydrogen-bonded N–H, and the broad bands at 3300–3330 cm^{-1} are assigned to internally hydrogen bonded N–H. Note that, as indicated in Figure 3, the integrated extinction coefficient for the non-hydrogen-bonded N–H stretch absorption varies inversely with temperature. Baseline corrections were applied to obtain the spectra shown.

Diamides **1–5** equilibrate between non-hydrogen-bonded and intramolecularly hydrogen bonded states in CH_2Cl_2 (1 mM) at 297 K, as judged by the presence of non-hydrogen-bonded (3450–3460 cm^{-1}) and hydrogen-bonded (3300–3350 cm^{-1}) signals in the N–H stretch region for each molecule. Diamide **6** does not experience internal hydrogen bonding under these conditions, within the limits of detection. Even though hydrogen-bonded and non-hydrogen-bonded N–H stretch signals have different extinction coefficients at maximum absorption, it is clear from these IR spectra that diamide **1** occurs predominantly in the intramolecularly hydrogen bonded state under these conditions but that diamides **2–5** exist largely in the non-hydrogen-bonded state.[14]

For diamides **1–3**, **5**, and **6**, cooling 1 mM CH_2Cl_2 solutions to 186 K (just above the CH_2Cl_2 freezing point) produces little qualitative change in the N–H stretch spectral region. Diamide **4**, however, experiences a dramatic increase in the amount of internal hydrogen bonding as the temperature is lowered. Variable-temperature IR spectral data from the N–H stretch region for diamides **3** and **4** are shown in Figure 1 to illustrate the

(7) Pimentel, G. C.; McClellan, A. L. *The Hydrogen Bond*; Freeman: San Francisco, 1960.

(8) Nēel, Marraud, and their co-workers have shown, in a long series of papers, that careful analysis of IR data can provide considerable insight on the internally hydrogen bonded states that are available to small peptides in solution. For leading references, see: (a) Nēel, J. *Pure Appl. Chem.* **1972**, *31*, 201. (b) Aubry, A.; Cung, M. T.; Marraud, M. *J. Am. Chem. Soc.* **1985**, *107*, 7640. None of the IR studies from these workers have involved variable-temperature measurements, as far as we know.

(9) (a) Urry, D. W.; Ohnishi, T. In *Peptides, Polypeptides and Proteins*; Blout, E. R., Bovey, F. A., Goodman, M., Lotan, N., eds.; Wiley-Interscience: New York, 1974; pp 230–247. (b) Urry, D. W.; Long, M. M. *CRC Crit. Rev. Biochem.* **1976**, *4*, 1.

(10) Rose, G. D.; Gierasch, L. M.; Smith, J. A. *Adv. Protein Chem.* **1985**, *37*, 1.

(11) (a) Kopple, K. D.; Ohnishi, M.; Go, A. *J. Am. Chem. Soc.* **1969**, *91*, 4264. (b) Ohnishi, M.; Urry, D. W. *Biochem. Biophys. Res. Commun.* **1969**, *36*, 194.

(12) For a review of IR studies of intramolecular hydrogen bonding in small molecules, see: Aaron, H. S. *Top. Stereochem.* **1980**, *11*, 1.

(13) Venkatachalapathi, Y. V.; Mierke, D. F.; Taulane, J. P.; Goodman, M. *Biopolymers* **1987**, *26*, 763.

(14) Diamide **1** is the only compound among **1–10** that displays three signals in the N–H stretch region in methylene chloride solution. In addition to the dominant broad signal at 3300 cm^{-1} (corresponding to an intramolecularly hydrogen bonded state) and the minor sharp signal at 3454 cm^{-1} (corresponding to the non-hydrogen-bonded state), there is a minor broad signal at 3430 cm^{-1}. The 3430-cm^{-1} signal could arise from an alternative internally hydrogen bonded state, in which the hydrogen bond is much weaker than the typical amide–amide hydrogen bond [perhaps involving the π system of the dimethylamide moiety as the acceptor (see ref 12)]. For a 1 mM solution of **1** in CCl_4, at room temperature, the 3300-cm^{-1} signal is again dominant in the N–H stretch region, but now the only other signal is a weak, broad band at 3430 cm^{-1}.

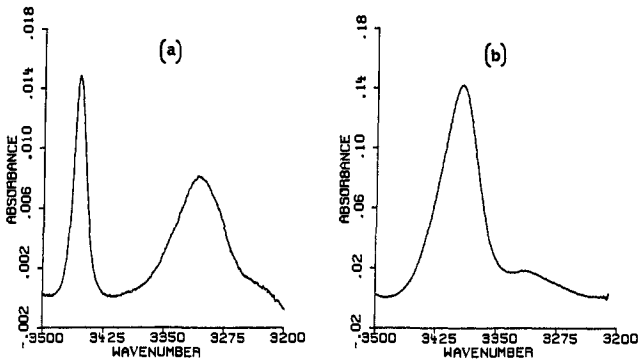

Figure 2. N–H stretch region FT-IR spectral data for diamide **4** at 235 K. (a) 1 mM in CH_2Cl_2 (absorption maxima at 3456 and 3310 cm^{-1}). (b) 10 mM in CH_3CN (absorption maxima at 3394 and 3320 cm^{-1}). In each case, the spectrum of the pure solvent, at 235 K, has been subtracted from the diamide spectrum. Baseline corrections were applied to obtain the spectra shown. Note the different vertical scales.

difference in behavior of these two molecules.

We examined the solution behavior of amide esters **7–10** to determine the effect of replacing a strong internal hydrogen bond acceptor (dimethylamide) with a weaker one (methyl ester).[15] At room temperature (297 K), the N–H stretch region of a 1 mM sample of amide ester **7** in CH_2Cl_2 shows two absorptions of similar

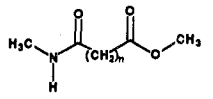

7, n = 1
8, n = 2
9, n = 3
10, n = 4

intensity, at 3453 and 3390 cm^{-1}. The latter signal represents an amide proton hydrogen bonded to an ester carbonyl. The relatively weak hydrogen bond accepting properties of the ester group are reflected in the fact that the frequency shift between non-hydrogen-bonded and hydrogen-bonded N–H signals is less than half as large for amide ester **7** as for analogous diamide **1**.[7,16] The IR spectra of amide esters **8–10** in CH_2Cl_2 show no sign of intramolecular hydrogen bonding at room temperature.

In CH_3CN, N–H stretch signals for amide protons not engaged in amide–amide hydrogen bonds occur around 3400 cm^{-1}. The shift in this value, relative to the 3450–3460-cm^{-1} range observed for solvated N–H stretch absorptions in CH_2Cl_2, results from hydrogen bonding with the nitrogen lone pair of electrons of CH_3CN. The nitrile is a much weaker hydrogen bond acceptor than an amide,[15a] as indicated by the fact that the N–H stretch absorption for *N*-methylacetamide's amide proton occurs at a substantially lower wavenumber (3320 cm^{-1}) when intermolecularly hydrogen bonded to another amide. At room temperature (297 K), a 10 mM acetonitrile solution of diamide **1** shows a very weak absorption for an intramolecularly hydrogen bonded amide proton (ca. 3300 cm^{-1}) and a strong absorption for a solvated N–H (3397 cm^{-1}). Under the same conditions, diamides **2–4** show absorptions only for N–H interacting with solvent (3406 cm^{-1}). Figure 2 shows the IR N–H stretch region spectra for a 1 mM sample of **4** in CH_2Cl_2 and for a 10 mM sample of **4** in CH_3CN, both at 237 K. It is clear, even at this low temperature, that intramolecular amide–amide hydrogen bonding is almost completely abolished by using CH_3CN as the solvent.

Quantification of Internal Hydrogen Bonding in Diamide 4 by IR. It is impossible to determine the extinction coefficient for either the internally hydrogen bonded N–H stretch or the solvated N–H stretch of diamide **4** in CH_2Cl_2, because the diamide experiences partial intramolecular hydrogen bonding at all temperatures in this solvent. In contrast, no intermolecular hydrogen bonding can be detected in a 1 mM CH_2Cl_2 solution of *N*-methylacetamide over the temperature range 186–297 K (−87 to +24 °C). Therefore, it is straightforward to determine the temperature dependence of the non-hydrogen-bonded N–H stretch band's integrated extinction coefficient (3500–3425 cm^{-1}) for this monoamide. (The data used to determine this function are shown graphically in Figure 3.) This integrated extinction coefficient allows us to estimate the concentration of non-hydrogen-bonded amide protons in a solution containing a known concentration of diamide **4** at a given temperature. By assuming that all other amide protons are intramolecularly hydrogen bonded, we can calculate the equilibrium constant relating the non-hydrogen-bonded and internally hydrogen bonded forms of **4** (eq 1). The temperature dependence of K_{eq} can then be used to construct a van't Hoff plot (eq 2).

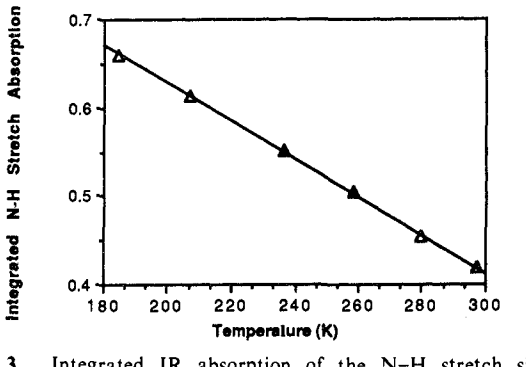

Figure 3. Integrated IR absorption of the N–H stretch signal (3500–3425 cm^{-1}) of a 1 mM solution of *N*-methylacetamide in CH_2Cl_2 (after solvent subtraction), as a function of temperature. The line corresponds to the function: $y = 1.057 - 0.00215x$. This function was used for determining the concentration of non-hydrogen-bonded N–H moieties in solutions of diamide **4**, as described in the text.

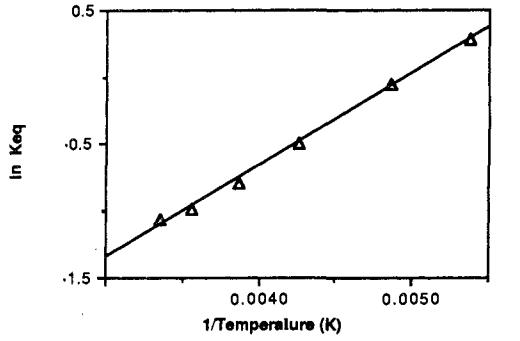

Figure 4. van't Hoff plot constructed from N–H stretch region IR data for diamide **4** in CH_2Cl_2, 186–297 K, as described in the text. The line was generated by using eq 2, $\Delta H° = -1.4$ kcal/mol and $\Delta S° = -6.8$ eu.

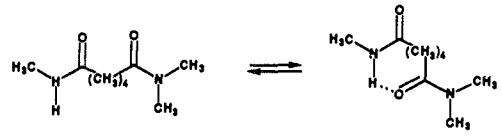

(1)

$$\ln K_{eq} = (-\Delta H°/R)(1/T) + \Delta S°/R \qquad (2)$$

The van't Hoff plot shown in Figure 4 implies that the internally hydrogen bonded state of **4** is enthalpically more favorable than the non-hydrogen-bonded state, in CH_2Cl_2, by 1.4 kcal/mol but entropically less favorable by 6.8 eu. (This analysis assumes that the enthalpic and entropic differences between the non-hydrogen-bonded and internally hydrogen bonded states are independent of temperature, i.e., that $\Delta C_p° = 0$ for the process shown in eq 1. The linearity of the van't Hoff plot in Figure 4, covering a 110 K range, is strong evidence for the validity of this assumption.[17])

The choice of a model compound for determining the temperature-dependent integrated extinction coefficient of the non-hydrogen-bonded N–H absorption is critical in the analysis above.[12] We carried out a second, completely parallel analysis

(15) (a) Arnett, E. M.; Mitchell, E. J.; Murty, T. S. S. R. *J. Am. Chem. Soc.* **1974**, *96*, 3875. (b) Spencer, J. N.; Garrett, R. C.; Moyer, F. J.; Merkle, J. E.; Powell, C. R.; Tran, M. T.; Berger, S. K. *Can. J. Chem.* **1980**, *58*, 1372.
(16) Pimentel, G. C.; McClellan, A. L. *Annu. Rev. Phys. Chem.* **1971**, 347.

(17) Stauffer, D. A.; Barrans, R. E.; Dougherty, D. A. *J. Org. Chem.* **1990**, *55*, 2762.

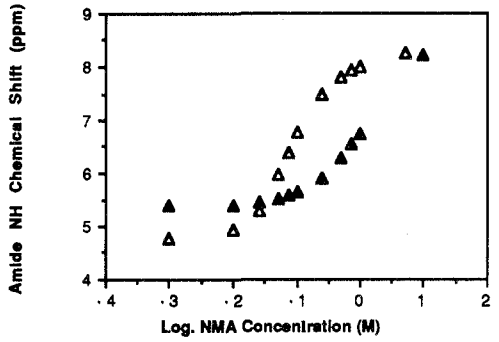

Figure 5. Amide proton NMR chemical shift of *N*-methylacetamide at room temperature, as a function of the logarithm of amide concentration, in CD_2Cl_2 (▲) and in 9:1 CCl_4/C_6D_6 (△).

of internal hydrogen bonding in diamide **4** in CH_2Cl_2 using the integrated extinction coefficient for the N–H stretch absorption of amide ester **10**. For **10**, as for *N*-methylacetamide, the integrated N–H stretch absorption varies linearly with temperature. There is no indication of intramolecular hydrogen bonding by **10** at any temperature. As before, the van't Hoff plot obtained for **4** by using **10** as the non-hydrogen-bonded reference is linear over a 110 K range (data not shown). The analysis based on **10** implies that the internally hydrogen bonded state of **4** is enthalpically more favorable than the non-hydrogen-bonded state, in CH_2Cl_2, by 1.6 kcal/mol, but entropically less favorable by 8.3 eu. Thus, replacing *N*-methylacetamide with **10** as the non-hydrogen-bonded reference leads to only relatively small differences in $\Delta H°$ and $\Delta S°$ values derived for eq 1. We regard these numerical differences as an indication of the level of uncertainty in the deduced thermodynamic parameters.

^{1}H NMR Spectroscopy.[18] Shown in Figure 5 are the amide proton chemical shifts of *N*-methylacetamide in CD_2Cl_2 and in 9:1 CCl_4/C_6D_6 plotted as a function of the logarithm of amide concentration. At low concentrations in each of these nonpolar solvents, the amide proton signal approaches a high-field limiting chemical shift (4.8 ppm in 9:1 CCl_4/C_6D_6 and 5.4 ppm in CD_2Cl_2), which presumably corresponds to the completely solvent exposed (non-hydrogen-bonded) amide proton. At high concentrations, the data obtained in 9:1 CCl_4/C_6D_6 approach a low-field limiting value of 8.4 ppm, which presumably corresponds to the fully amide–amide hydrogen bonded state. There is no leveling off in the CD_2Cl_2 data, but δNH = 8.4 ppm for the most concentrated sample, 10 M. Since pure *N*-methylacetamide is 13.1 M, we assume that the limiting value for the fully hydrogen bonded amide proton is roughly the same in CD_2Cl_2 as in 9:1 CCl_4/C_6D_6.

Klotz and Franzen deduced a dimerization constant of 4.7 M^{-1} for *N*-methylacetamide in CCl_4 by analyzing the first overtones (near-IR) of the hydrogen-bonded and non-hydrogen-bonded N–H stretch signals at various concentrations at room temperature and then extrapolating their data to infinite dilution to eliminate the effects of higher order aggregation.[19] An analogous treatment of the NMR data (9:1 CCl_4/C_6D_6) shown in Figure 5 gives the same value. The dimerization constant calculated from the CD_2Cl_2 data shown in Figure 5 is 0.8 M^{-1}. This comparison suggests that amide–amide hydrogen bonding is less favorable in the more polar solvent (dielectric constants: carbon tetrachloride, 2.2; benzene, 2.3; methylene chloride, 8.9), a result that is consistent with other observations in the literature.[15a,19,20]

Figure 6 shows the temperature dependences of the amide proton chemical shifts of diamides **1–6** in CD_2Cl_2 (all samples 1 mM). Also shown are data for an equimolar mixture of *N*-methylacetamide and *N*,*N*-dimethylacetamide (1 mM each). This

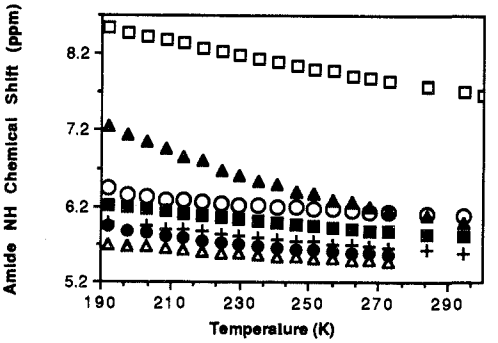

Figure 6. Amide proton NMR chemical shifts of diamides **1–6** and a 1:1 mixture of *N*-methylacetamide and *N*,*N*-dimethylacetamide, as a function of temperature. Data were obtained in CD_2Cl_2; all amides were at 1 mM concentration. Diamide **1** (□); diamide **2** (○); diamide **3** (■); diamide **4** (▲); diamide **5** (+); diamide **6** (●); 1:1 mixture of monoamides (△).

Table I. Amide Proton NMR Chemical Shift Temperature Dependences (ppm/K) for Diamides **1–6** in CD_2Cl_2 and in 9:1 CCl_4/C_6D_6(CTB)[a]

diamide	$\Delta\delta/\Delta T$ (CD_2Cl_2)[b]	$\Delta\delta/\Delta T$ (9:1 CTB)[c]
1	−0.0076	−0.0050
2	−0.0025	−0.0079
3	−0.0036	−0.0079
4	−0.0100	−0.0130
5	−0.0036	
6	−0.0033[e]	
monoamides[d]	−0.0025[e]	−0.0039

[a] All amides 1 mM. Data were obtained on a Bruker AM-500 spectrometer as described under Experimental Section. [b] 220–305 K, unless otherwise indicated. [c] 300–355 K. [d] 1:1 mixture of *N*-methylacetamide and *N*,*N*-dimethylacetamide, 1 mM each. [e] 220–275 K.

monoamide mixture serves as a control for any onset of intermolecular hydrogen bonding as the temperature is lowered. [Intermolecular interactions must be minimal even at the lowest temperatures, because the chemical shift differences between the 1 mM monoamide mixture and a CD_2Cl_2 solution containing only 1 mM *N*-methylacetamide are miniscule at these temperatures (ca. 0.05 ppm).] The NMR data in Figure 6 are consistent with the qualitative picture provided by the variable-temperature IR data discussed above. In particular, diamide **1** experiences considerably more internal hydrogen bonding than any other of the diamides, and the internal hydrogen bonding in diamide **4** shows a uniquely large temperature dependence.

Table I shows the "reduced temperature coefficients" ($\Delta\delta/\Delta T$) derived from the variable-temperature NMR data for **1–6** in CD_2Cl_2. (The reduced temperature coefficient has become a standard parameter in the characterization of peptide behavior in solution.[21]) Also shown in Table I are $\Delta\delta/\Delta T$ values obtained in 9:1 CCl_4/C_6D_6 for diamides **1–4**. (These latter data were obtained for 1 mM samples over the range 300–355 K; at lower temperatures, intermolecular hydrogen bonding begins to occur in this solvent system.) Comparison of the data sets from CD_2Cl_2 and 9:1 CCl_4/C_6D_6 suggests that the intramolecular hydrogen bonding behavior of the diamide series is qualitatively similar in these two relatively noninteractive solvents.

In CD_3CN, the amide proton chemical shift of *N*-methylacetamide is independent of amide concentration below 100 mM, and the high-field limiting chemical shift (dilute solutions) is 6.2 ppm, at room temperature. The weaker tendency for intermolecular amide–amide hydrogen bonding and the higher limiting amide proton chemical shift in CD_3CN, relative to CD_2Cl_2 and 9:1 CCl_4/C_6D_6, presumably reflect the hydrogen-bonding competition offered by the solvent nitrile. The greater polarity of acetonitrile may also contribute to diminished hydrogen-bond-mediated aggregation in this solvent (dielectric constant of acetonitrile = 38.8).

(18) Monoamide aggregation in $CDCl_3$ and CCl_4 has been previously been quantified by monitoring the amide proton chemical shift. See: (a) LaPlanche, L. A.; Thompson, H. B.; Rogers, M. T. *J. Chem. Phys.* **1965**, *69*, 1482. (b) Graham, L. L.; Chang, C. Y. *J. Phys. Chem.* **1971**, *75*, 776.

(19) (a) Klotz, I. M.; Franzen, J. S. *J. Am. Chem. Soc.* **1962**, *84*, 3461. (b) See also: Krikorian, S. E. *J. Phys. Chem.* **1982**, *86*, 1875.

(20) Franzen, J. S.; Stephen, R. E. *Biochemistry* **1963**, *2*, 1321.

(21) Kessler, H. *Ang. Chem., Int. Ed. Engl.* **1982**, *21*, 512.

Table II. Amide Proton NMR Chemical Shift Temperature Dependences (ppm/K) for Diamides **1–4** in CD_3CN, 250–330 K[a]

diamide	$\Delta\delta/\Delta T$	δNH at 298 K
1	−0.0022	7.06
2	−0.0024	6.34
3	−0.0031	6.26
4	−0.0039	6.38
monoamides[b]	−0.0035	6.23

[a] All amides 10 mM. Data were obtained on a Bruker AM-500 spectrometer as described under Experimental Section. [b] 1:1 mixture of *N*-methylacetamide and *N*,*N*-dimethylacetamide, 10 mM each.

Table III. Amide Proton NMR Chemical Shift Temperature Dependences (ppm/K) for Amide Esters **7–10** in CD_2Cl_2, 190–280 K[a]

amide ester	$\Delta\delta/\Delta T$	δNH at 263 K
7	−0.0060	6.92
8	−0.0018	5.61
9	−0.0022	5.52
10	−0.0032	5.55
NMA[b]	−0.0027	5.49

[a] All compounds 1 mM. Data were obtained on a Bruker AM-500 spectrometer as described under Experimental Section. [b] *N*-Methylacetamide.

Table II shows $\Delta\delta/\Delta T$ values for diamides **1–4** and for a 1:1 mixture of *N*-methylacetamide and *N*,*N*-dimethylacetamide in CD_3CN (all components 10 mM; there appears to be no intermolecular amide–amide hydrogen bonding at this concentration in CD_3CN, because identical $\Delta\delta/\Delta T$ data sets are obtained with 5 and 10 mM diamide samples). Also shown are δNH values measured at 298 K. The data for diamides **2–4** closely parallel the data for the 1:1 monoamide mixture over the entire temperature range, in terms of both chemical shift and temperature dependence, suggesting that little or no intramolecular hydrogen bonding occurs in these molecules in CD_3CN. The δNH of diamide **1** is shifted downfield relative to the other diamides at all temperatures, which is consistent with existence of some internal hydrogen bonding in the six-membered ring in CD_3CN. These NMR results are generally consistent with the IR data obtained in CH_3CN discussed above.

Table III shows $\Delta\delta/\Delta T$ values for 1 mM samples of amide esters **7–10** and a 1 mM sample of *N*-methylacetamide in CD_2Cl_2 (190–280 K). Also shown are δNH values for all samples at 263 K. The data sets for amide esters **8–10** are very similar to that for *N*-methylacetamide, in terms of both temperature dependence and absolute chemical shift. This similarity suggests that little or no intramolecular hydrogen bonding occurs in **8–10** under these conditions. For amide ester **7** δNH occurs more than 1.0 ppm downfield from δNH of the other samples at all temperatures. The temperature dependence of δNH (−0.0060 ppm/K) is larger for **7** than for any other amide ester but smaller than for the analogous diamide **1** (−0.0076 ppm/K) in CD_2Cl_2. These NMR observations are consistent with the room temperature IR data in indicating that **7**, unlike the other amide esters, experiences a significant amount of intramolecular hydrogen bonding in methylene chloride solution.

Quantification of Internal Hydrogen Bonding in Diamide 4 by ^{1}H NMR. For an amide proton equilibrating between a non-hydrogen-bonded state and a hydrogen-bonded state, the equilibrium constant for the two-state system may be extracted from δNH if the limiting chemical shifts for the non-hydrogen-bonded and hydrogen-bonded states are known (eq 3). (In eq 3, δ_{obs} is

$$K_{eq} = (\delta_{obs} - \delta_n)/(\delta_b - \delta_{obs}) \quad (3)$$

the observed chemical shift, δ_n is the limiting chemical shift for the non-hydrogen-bonded state, and δ_b is the limiting chemical shift for the fully hydrogen bonded state.) Determining the equilibrium constant at several temperatures allows one to evaluate $\Delta H°$ and $\Delta S°$ for the two-state process, via van't Hoff analysis (eq 2).

Table IV. Results of van't Hoff Analyses (eq 2) for Diamide **4** in CD_2Cl_2, 220–275 K, as a function of the Temperature Dependence Used for δ_b (eq 3)[a]

$\Delta\delta_b/\Delta T$, ppm/K	$\Delta H°$, kcal/mol	$\Delta S°$, eu
0	−1.2	−7.0
−0.005	−1.5	−8.0
−0.010	−1.9	−9.2

[a] The second row is our best estimate for a fully hydrogen bonded amide NH. The van't Hoff plot obtained for this intermediate value of δ_b is shown in Figure 6.

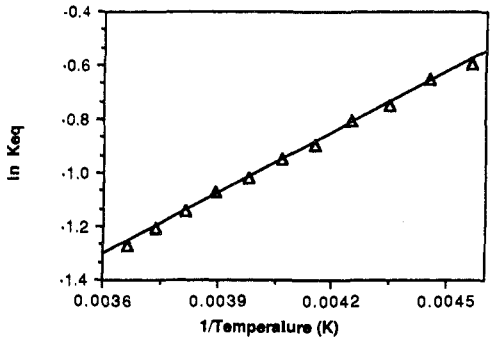

Figure 7. van't Hoff plot constructed from amide proton NMR chemical shift data for diamide **4** in CD_2Cl_2, 220–275 K, as described in the text. The line was generated by using eq 2, $\Delta H°$ = −1.5 kcal/mol and $\Delta S°$ = −8.0 eu.

In CD_2Cl_2, the amide proton chemical shift for the equimolar mixture of *N*-methylacetamide and *N*,*N*-dimethylacetamide can serve as δ_n at all temperatures. Determining the limiting chemical shift for the intramolecularly hydrogen bonded state is more problematic, because both the absolute value and the temperature dependence of δ_b may vary with hydrogen bond geometry. (The different covalent juxtapositions of the hydrogen bond donor and acceptor in diamides **1–6** should lead to hydrogen bonds of diverse geometries.) We estimate the required value of δ_b at room temperature from the upper limiting δNH in concentrated *N*-methylacetamide solutions (8.4 ppm) and assume that this value applies to a hydrogen bond of optimum geometry. For the temperature *dependence* of a geometrically optimally hydrogen bonded proton, we believe a good estimate to be the $\Delta\delta/\Delta T$ value (−0.0050 ppm/K) observed for a triamide that appears to be locked in a linear intramolecular hydrogen bond at all temperatures in methylene chloride.[22]

Table IV shows the results of three NMR-based van't Hoff analyses for diamide **4** in CD_2Cl_2 over the temperature range 220–275 K. For each of these analyses, a different temperature dependence for δ_b has been used. The middle row of numbers results from the use of the value that we believe to be most accurate (−0.0050 ppm/K); the first row corresponds to the assumption that δ_b has no temperature dependence, and the third row corresponds to the assumption that δ_b has twice the expected temperature dependence (−0.010 ppm/K). Figure 7 shows the van't Hoff plot for the δ_b value we believe to be accurate. This analysis implies that the intramolecularly hydrogen bonded state is 1.5 kcal/mol more favorable enthalpically than the non-hydrogen-bonded state, but 8.0 eu less favorable entropically, in

(22) The compound we use to estimate $\Delta\delta/\Delta T$ for an amide proton locked in an optimal geometry hydrogen bond is triamide **4** in ref 6a. We noted there that the IR spectrum of this triamide (1 mM) shows a tiny signal for a non-hydrogen-bonded NH stretch in CH_2Cl_2 at room temperature, but we believe that this signal derives exclusively from the minor rotamer (**4b** in ref 6a), which has the *E* configuration about the central C–N bond. Consistent with our hypothesis that the major rotamer of that triamide is completely intramolecularly hydrogen bonded at all temperatures in methylene chloride is our observation that δNH for the major rotamer is concentration independent, but δNH for the minor rotamer increases in more concentrated samples. We cannot use data from this triamide to provide the absolute value for δNH of a completely hydrogen bonded amide proton because the conformation we have proposed for the major rotamer of this molecule in methylene chloride places the lone amide in the shielding cone of the central group's π system.

CD_2Cl_2 solution. These values for $\Delta H°$ and $\Delta S°$ are consistent with the values deduced independently from variable-temperature IR data obtained in CH_2Cl_2. Since the $\Delta H°$ and $\Delta S°$ values given in the first and third rows of Table IV correspond to unrealistically extreme assumptions, these numbers provide very generous indications of the level of uncertainty in our NMR-based thermodynamic analysis.

Discussion

The data we have presented are significant for two reasons. (1) Changes in behavior across the series **1–6** allow us to examine how the conformation-directing effect of a single intramolecular amide–amide hydrogen bond is modulated by incremental variation in the covalent spacing between donor and acceptor and by solvent properties. (2) Variable-temperature ^1H NMR and IR measurements provide independent probes of the thermodynamic relationship between the family of conformations in which an intramolecular hydrogen bond exists and the family of conformations in which the amide proton is fully solvated.

Interpretation of Amide Proton $\Delta\delta/\Delta T$ Data. Variable-temperature NMR measurements have been widely used to study the internal hydrogen bonding experienced by amide protons in peptides and proteins,[9,10] but this type of measurement has not previously been correlated with variable-temperature IR data. Our work demonstrates for the first time that the amide proton chemical shift temperature dependence ($\Delta\delta/\Delta T$) can provide thermodynamic information on intramolecular hydrogen bonding. These results therefore provide an important benchmark for the interpretation of $\Delta\delta/\Delta T$ data obtained with more complex peptides.

The present findings require a modification of the accepted rules for interpreting amide proton $\Delta\delta/\Delta T$ data obtained in nonpolar solvents. Small $\Delta\delta/\Delta T$ values have generally been associated with amide protons that are completely locked in an intramolecular hydrogen bond or completely free of hydrogen bonding over the temperature range examined.[23,24] We have now shown that an amide proton displaying a small chemical shift temperature dependence can be equilibrating between internally hydrogen bonded and non-hydrogen-bonded states (e.g., diamides **2** and **3** in methylene chloride); this situation arises when the enthalpy difference between internally hydrogen bonded and completely solvent exposed states is small.

In each diamide, the net energetic gain associated with intramolecular hydrogen bond formation must compete with various factors that oppose hydrogen-bonded ring closure. Before we examine the balance of forces that obtains in each molecule, we must review several issues that pertain to the entire series.

Hydrogen Bond Geometry. The enthalpic contribution of the intramolecular hydrogen bond depends on the spatial juxtaposition of the donor and acceptor.[25] Statistical surveys of crystallographic data suggest that optimum bond distances are approximately 1.9 Å for H--O and 2.9 Å for N--O (the latter value becomes important when the proton cannot be located).[26] Ab initio calculations imply that amide–amide hydrogen bonding is strongest when the N–H--O angle approaches linearity (optimum values are calculated to be around 160°); hydrogen bond energy appears to be less sensitive to the C=O--H angle, however, as long as that angle is greater than 90°.[25-27] Deviations from a planar arrangement (i.e., non-planarity about the N–C=O--H torsion angle) are energetically unfavorable.

Enthalpic Forces Opposing Internal Hydrogen Bond Formation. The hydrogen bond enthalpy cannot offset the energetic cost of even small distortions in covalent bond lengths or angles. Therefore, we can be certain that the internally hydrogen bonded conformations available to diamides **1** and **2** do not involve optimum hydrogen bond geometries, because the six- and seven-membered rings will not tolerate N–H--O angles that approach linearity. On the other hand, the amide–amide hydrogen bond enthalpy is sufficient to overcome a certain amount of torsional strain and longer range nonbonded repulsion, which means that a conformation containing an amide–amide hydrogen bond of optimal geometry can be enthalpically favorable, relative to non-hydrogen-bonded conformations, even if a few gauche interactions are induced as the covalent connector bends back upon itself.

Conformational Entropy. The loss of conformational freedom should lead to an increasing entropic barrier to intramolecular hydrogen bond formation across the series **1–6**. Each extra methylene in the connecting segment corresponds to an additional carbon–carbon single bond, the motion of which must be restricted when an internal hydrogen bond forms. Enthalpic and entropic factors are not necessarily completely distinct in these molecules, however. An optimal hydrogen-bonding interaction occurs only in a highly restricted subset of all possible donor–acceptor juxtapositions, which means that the most enthalpically favorable hydrogen bond geometries are entropically disfavored relative to suboptimal but more numerous (i.e., less spatially restrictive) hydrogen bond geometries.

Solvent Effects. Both the polarity and the hydrogen-bonding capacity of the solvent influence the conformation-directing role of the internal hydrogen bond in a given diamide. If the solvent forms strong hydrogen bonds, then the enthalpic gain attendant upon internal hydrogen bond formation will be severely diminished or abolished, because the internal hydrogen bond forms at the expense of at least one hydrogen bond to solvent. The polarity of the solvent can also modulate the enthalpic gain associated with internal hydrogen bond formation, since the hydrogen bond interaction has a substantial electrostatic component (hydrogen bond energy decreases in more polar environments). Klotz and Franzen concluded that the hydrogen-bonding capacity of the solvent, rather than solvent polarity, exerts the dominant influence on amide–amide hydrogen bonding, on the basis of their observation that intermolecular hydrogen bonding between *N*-methylacetamide molecules is significantly more favorable in CCl_4 than in dioxane, even though both solvents have dielectric constants of 2.2.[19a,28] (The oxygen atoms of the dioxane molecule are reasonably strong hydrogen bond acceptors, but the chlorine atoms of CCl_4 are, at best, extremely weak acceptors.)

We have shown that changing solvent from methylene chloride to acetonitrile substantially reduces intramolecular hydrogen bonding in diamides **1–4**, as indicated by both NMR and IR data. These observations are consistent with those of Klotz and Franzen on the ability of hydrogen-bonding solvents like dioxane and water to disrupt intermolecular amide–amide hydrogen bonding.[19a] On the basis of their findings, Klotz and Franzen argued that formation of intramolecular amide–amide hydrogen bonds should not contribute to the enthalpic driving force for protein folding in water, because the folding process simply exchanges water–amide hydrogen bonds for hydrogen bonds between amide groups on the protein and water–water hydrogen bonds.[19a,29] (In the context of this argument, intramolecular amide–amide hydrogen bonds can still provide a *structure-specifying force* within the collapsed peptide chain, influencing the relative stabilities of alternative folded states.[4b] Amide groups buried in the core of the folded protein are prevented from hydrogen bonding with bulk water; therefore, folded conformations that leave buried hydrogen bond donors and acceptors isolated from one another are disfavored relative to conformations in which donors and acceptors are paired.)

Diamide 1. This smallest diamide is the only member of the series to exist predominantly in the intramolecularly hydrogen

(23) Stevens, E. S.; Sugawara, N.; Bonara, G. M.; Toniolo, C. *J. Am. Chem. Soc.* **1980**, *102*, 7048.
(24) Riberio, A. A.; Goodman, M.; Naider, F. *Int. J. Pept. Protein Res.* **1979**, *14*, 414.
(25) Peters, D.; Peters, J. *J. Mol. Struct.* **1980**, *68*, 255.
(26) Baker, E. N.; Hubbard, R. E. *Prog. Biophys. Mol. Biol.* **1984**, *44*, 97.
(27) Mitchell, J. B. O.; Price, S. L. *Chem. Phys. Lett.* **1989**, *154*, 267.
(28) Subsequent ^1H NMR studies in CCl_4 and dioxane have been consistent with Klotz and Franzen's near-IR-based conclusions. See: (a) ref 18b. (b) Graham, L. L.; Chang, C. Y. *J. Phys. Chem.* **1971**, *75*, 784.
(29) For a review of current theories on the roles of internal hydrogen bonding and other noncovalent forces in protein folding and the historical development of those theories, see: Dill, K. D. *Biochemistry* **1990**, *29*, 7133.

bonded state at room temperature in methylene chloride. The six-membered ring interaction is distinctive also in that some internal hydrogen bonding remains when the hydrogen-bond-accepting nature of the solvent is strengthened (**1** in acetonitrile) or the internal acceptor is weakened (amide ester **7**). These same changes completely abolish intramolecular interaction when the hydrogen-bonded ring is seven-membered or larger. In the six-membered ring, the internal hydrogen bond cannot achieve an optimal geometry, because the N–H--O angle is constrained to be less than 140°. The energetic favorability of the six-membered-ring hydrogen-bonded state probably results in part from the lack of torsional strain opposing the closure of the hydrogen-bonded ring and from the minimal entropic barrier to internal hydrogen bond formation.

Diamide 2. Both IR and NMR measurements show that there is a small but fairly constant amount of internal hydrogen bonding in **2** over a large temperature range in methylene chloride, implying that the non-hydrogen-bonded and intramolecularly hydrogen bonded states are of similar enthalpy. Apparently, the enthalpic gain associated with seven-membered-ring amide–amide hydrogen bond formation in methylene chloride is largely counterbalanced by torsional strain induced by ring closure. Framework molecular models suggest that the covalent juxtaposition of hydrogen bond donor and acceptor in diamide **2** precludes an internal hydrogen bond that approaches linearity in its N–H--O angle or planarity in its N–C=C--H arrangement. Therefore, it is not surprising that the seven-membered-ring hydrogen bond does not exert a powerful conformation-directing effect.

Changing solvents alters the internal balance of conformation-directing forces. In the less polar medium 9:1 CCl_4/C_6D_6, the hydrogen bond should be more favorable enthalpically, but the torsional strain opposing ring closure should not change. Indeed, in this solvent system, the temperature dependence of δNH for **2** is substantially larger (in an absolute sense) than for the control mixture of *N*-methylacetamide and *N*,*N*-dimethylacetamide, while the corresponding values are nearly equal in CD_2Cl_2 (Table II). On the other hand, in acetonitrile, which can compete with the dimethylamide moiety of **2** for hydrogen bond acceptance, no evidence of an intramolecular hydrogen bond is found by IR or NMR (Table III). If, instead of moving to a more polar solvent, we reduce the enthalpic advantage of the internally hydrogen bonded state by exchanging the dimethylamide moiety of **2** for the methyl ester of **8**, we observe the same result: internal hydrogen bonding disappears.

Diamide 3. The behavior of **3** parallels that of **2**. In methylene chloride, the internally hydrogen bonded and non-hydrogen-bonded states appear to be of similar enthalpy, and the energetic difference between these two states responds similarly to changes in solvent or internal hydrogen bond acceptor. Framework models suggest that **3** is the smallest diamide in which a geometrically optimal

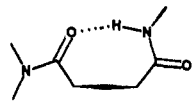

3

amide–amide hydrogen bond is possible. The models also reveal, however, that achievement of a linear N–H--O arrangement requires the two CH_2—CH_2 bonds in the connecting segment to approach eclipsed conformations. In *n*-butane, the analogous eclipsed conformation (methyls eclipsing hydrogens) is calculated to be 3.3 kcal/mol higher in energy than the anti conformational ground state.[30] The data of Klotz and Franzen suggest that the maximum enthalpic gain from formation of a geometrically optimal intramolecular hydrogen bond in CCl_4 is about 4 kcal/mol;[19a] the corresponding value in methylene chloride is probably somewhat smaller. Formation of an intramolecular amide–amide hydrogen bond of optimal geometry is therefore unlikely to overcome two severe eclipsing interactions in the linker of **3**. The internal hydrogen bonding detected in the less polar solvents for **3** presumably occurs in nonoptimal geometries, and the enthalpy gained by intramolecular hydrogen bond formation is offset by torsional strain induced in the linking segment.

Diamide 4. In both chlorocarbon solvents, intramolecular hydrogen bonding in **4** shows the largest sensitivity to changes in temperature of all the diamides. The substantial increase in internal hydrogen bonding that occurs as the temperature is lowered implies that the intramolecularly hydrogen bonded state of **4** is significantly more favorable enthalpically than the non-hydrogen-bonded state. Independent quantitative analyses of variable-temperature NMR and IR data indicate that the internally hydrogen bonded state is 1.4–1.6 kcal/mol more enthalpically stable than the state involving amide NH solvation by methylene chloride.

Molecular models suggest that the nine-membered ring conformation of **4** can accommodate a geometrically favorable hydrogen bond donor–acceptor orientation with minimal torsional strain in the linking segment. A linear N–H--O angle is compatible with an anti torsion angle about the central CH_2—CH_2 bond of the butyl chain linking the two carbonyl carbons and gauche torsion angles about the other two CH_2—CH_2 bonds, as indicated in the drawing. The gauche conformation of *n*-butane is about 0.8 kcal/mol higher in energy than the anti conformation,[30] but the two gauche interactions in the proposed internally hydrogen bonded state of **4** should be less sterically demanding

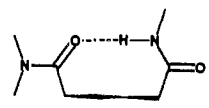

4

than that in butane itself, since one of the interacting carbons is sp^2 in each case. The deduced 1.4–1.6 kcal/mol enthalpic stability of the internally hydrogen bonded state of **4** in methylene chloride is consistent with the net effect expected from a hydrogen bond enthalpy of −2 to −3 kcal/mol opposed by two modest gauche interactions.

The stability of the internally hydrogen bonded state relative to the non-hydrogen-bonded state disappears when **4** is placed in acetonitrile and when the dimethylamide acceptor is replaced with a methyl ester (**10**). Both of these observations imply that the cyclically hydrogen bonded state is favored by the enthalpic gain associated with formation of the hydrogen bond itself and is not simply a byproduct of other conformation-directing forces.

NMR and IR data suggest that the nine-membered ring internally hydrogen bonded state of **4** is less favorable entropically than the non-hydrogen-bonded state in methylene chloride by 6.8–8.3 eu. On the basis of their survey of reactions in which small and medium-sized rings are closed by formation of a *covalent* bond, Page and Jencks have proposed that 4.5 eu is "a representative value for the entropy that may be lost upon freezing an internal rotation, in the absence of compensating factors".[31] In **4**, there are five single carbon–carbon bonds that must suffer some restriction of rotation upon hydrogen-bonded ring closure, which might suggest that the loss of internal rotational entropy resulting from nine-membered ring formation should be in excess of 20 eu. The relatively small net entropic cost of hydrogen-bonded ring closure indicated by our data may reflect residual entropy in the stretching vibrational mode of the O--H hydrogen bond and in low-frequency motions of the hydrogen-bonded ring.[31] Differences in the solvation of internally hydrogen bonded and non-hydrogen-bonded forms of **4** may also affect $\Delta S°$.

Diamides 5 and 6. At room temperature in methylene chloride, only a small amount of internal hydrogen bonding can be detected in dilute solutions of **5** and none at all in **6**. Although a small amount of intramolecular hydrogen bonding does appear in **6** as the temperature is decreased, even at the lowest temperatures both of these diamides are overwhelmingly non hydrogen bonded in

(30) Allinger, N. L.; Yuh, Y. H.; Lii, J. H. *J. Am. Chem. Soc.* **1989**, *111*, 8551, and references cited therein.

(31) Page, M. I.; Jencks, W. P. *Proc. Natl. Acad. Sci. U.S.A.* **1971**, *68*, 1678.

methylene chloride. Molecular models suggest that formation of a geometrically favorable intramolecular amide–amide hydrogen bond in the 10-membered ring of **5** or the 11-membered ring of **6** cannot occur without concomitant eclipsing interactions along the covalent backbone and transannular steric repulsions. Furthermore, in both cases, the entropic barrier to hydrogen-bonded ring closure may be large enough that the enthalpic gain associated with internal hydrogen bond formation cannot enforce a folded conformation at accessible temperatures.

Conclusions. Diamides **1–6** provide an excellent opportunity for scrutinizing the conformation-directing effects of a single intramolecular amide–amide hydrogen bond. As the length of the covalent connection between the donor and acceptor groups is varied, the changing enthalpic relationship between the internally hydrogen bonded and non-hydrogen-bonded states of these diamides in chlorocarbon solvents reveals that the drive for hydrogen bond formation is delicately balanced against torsional strain and the other unfavorable noncovalent interactions that develop as the donor and acceptor approach one another.[32] Particularly striking is the observation of a substantial enthalpic conformation-directing effect when the amide–amide hydrogen bond occurs in a 9-membered ring (diamide **4**), but the lack of such an effect in the 7-, 8-, 10-, and 11-membered rings. Not surprisingly, the ability of an internal amide–amide hydrogen bond to enforce folded conformations in these flexible molecules is strongly dependent upon the nature of the medium.

This study is our first step toward elucidating the network of noncovalent forces that stabilize folded protein conformations. Competition between hydrogen bond enthalpy and the enthalpic and entropic forces that oppose hydrogen-bonded ring closure must also occur, on a much larger scale, in the core of a folded protein. It is interesting to note that peptide reverse turns often contain hydrogen bonds in 7-membered rings (γ-turns) or 10-membered rings (β-turns), while 6- and 9-membered ring amide–amide hydrogen bonds can occur in proteins only if a side-chain amide group (from asparagine or glutamine) is involved. Because the covalent connectivities between amide groups in diamides **1–6** are not those found in peptides, however, our observations on the relationship between hydrogen-bonded ring size and the energetic favorability of the internally hydrogen bonded state are not directly applicable to peptide and protein conformation. (We are currently examining the energetic favorability of small- and medium-sized hydrogen bonded rings in peptides.)

The data we have generated on intramolecular hydrogen bonding in simple model compounds should be helpful for evaluating the various molecular mechanics programs that are used to predict peptide and protein conformations.[33] Any computational approach that cannot reproduce the behavior of diamides **1–6** is unlikely to provide realistic information on biopolymers. Empirical data on our molecules and related model compounds may ultimately be useful in parametrizing the hydrogen-bonding potential functions and solvation subroutines employed in such programs. We are currently evaluating commercially available computational tools for their abilities to reproduce our observations.

Our parallel variable-temperature NMR and IR studies of internal hydrogen-bonding equilibria in the homologous diamides **1–6** have revealed two points that are directly relevant to peptide conformational analysis. (1) If limiting NMR chemical shifts (and the temperature dependences of those chemical shifts) are known for the internally hydrogen bonded and non-hydrogen-bonded (fully solvated) states experienced by an amide proton, $\Delta H°$ and $\Delta S°$ for the equilibrium between the two states can be determined from amide proton $\Delta\delta/\Delta T$ data. Even if the limiting chemical shift values are not accurately known, qualitative insights on the enthalpic and entropic relationships between these states may be available from δNH and $\Delta\delta/\Delta T$ data. (2) In non-hydrogen-bonding solvents, amide protons can exhibit small temperature dependences even if they are equilibrating between hydrogen-bonded and non-hydrogen-bonded states, provided the two states are of similar enthalpy. Distinguishing this situation from a completely non hydrogen bonded or a fully internally hydrogen bonded case can be rigorously accomplished through the use of IR data with simple molecules. With more complex molecules, absolute amide proton chemical shift data may be useful for making educated guesses among these three possibilities.

Experimental Section

All melting points are uncorrected. THF was freshly distilled from sodium benzophenone ketyl under N_2. Routine ^{1}H NMR spectra (for characterization) were obtained on a Bruker WP-200 spectrometer. FT-IR spectra were obtained on a Nicolet 740 instrument. Amide N–H stretch absorptions in the non-hydrogen-bonded region (3450–3460 cm^{-1}) were sharp and maxima could be determined reliably to within 2 cm^{-1}; N–H stretch signals in the hydrogen-bonded region (below 3430 cm^{-1}) were broad, and absorption maxima could be determined only to within 10 cm^{-1}. Routine NMR and IR data reported below for compound characterization were obtained at room temperature. High-resolution electron impact ionization mass spectroscopy was performed on a Kratos MS-80. Commercially obtained starting materials were used without further purification. Column chromatography was carried out by using low N_2 pressure with 230–400-mesh silica gel 60 from EM Science. Columns eluted with low percentages of MeOH in CH_2Cl_2 or $CHCl_3$ were slurry-packed after the slurry had been stirred with the eluant for at least an hour. Fresh solvent was then passed through the column continuously until subtle changes in the gray hue of the silica had moved completely through the column bed (for 2% MeOH or less, this preequilibration of the column could be quite time-consuming). This preequilibration was essential for optimal resolution.

***N,N,N'*-Trimethylpropanediamide (1).** To 25 mL of 40 wt % aqueous dimethylamine (0.2 mol) was added 7.2 g (0.05 mol) of solid Meldrum's acid. The resulting solution was allowed to stand for 63 h and then cooled to 0 °C. The solution was acidified by cautious addition of 12 mL of concentrated HCl and then extracted with 20 20-mL portions of $CHCl_3$. The combined organic layers were dried over Na_2SO_4 and evaporated to give 5.28 g (81%) of the mono-*N,N*-dimethylamide of malonic acid as a tan waxy solid (very hygroscopic): ^{1}H NMR ($CDCl_3$) δ 3.06 (s, 3 H, NCH_3), 3.07 (s, 3 H, NCH_3), 3.39 (s, 2 H, CH_2). This material was carried on without further purification.

N-Hydroxybenzotriazole hydrate (0.6 g, ca. 3.6 mmol) was azeotropically dried with toluene and then placed in a round-bottom flask under N_2 along with 0.39 g (3 mmol) of mono-*N,N*-dimethylamide of malonic acid. These solids were dissolved in 15 mL of THF, and 0.75 g (3.6 mmol) of dicyclohexylcarbodiimide was added. A white precipitate quickly developed. After 2 h, the slurry was filtered through a glass frit under positive N_2 pressure. The filtrate was cooled to 0 °C, and gaseous CH_3NH_2 was bubbled through for 10 min. The reaction vessel was then allowed to warm to room temperature (under a positive pressure of N_2). The crude product was chromatographed on a SiO_2 column eluting with 5% MeOH in CH_2Cl_2 to give the desired diamide as an off-white solid (0.37 g, 85%), small portions of which were further purified by sublimation: mp 97–98 °C; ^{1}H NMR ($CDCl_3$) δ 2.81 (d, J = 4.9 Hz, 2 H, NHCH_3), 2.98 (s, 3 H, NCH_3), 3.08 (s, 3 H, NCH_3), 3.32 (s, 2 H, CH_2), 7.86 (broad, 1 H, NH); IR (1 mM in CH_2Cl_2) 3454 (NH), 3430 (broad, NH), 3300 (broad, NH), 1672 (C=O), 1633 (C=O) cm^{-1}. EI MS *m/e*: 144.0888. Calcd for $C_6H_{12}N_2O_2$: 144.0899.

***N,N,N'*-Trimethylbutanediamide (2).** To a mixture of 10 mL of 40 wt % aqueous dimethylamine (0.08 mol) and 10 mL of H_2O was added 4.0 g (0.04 mol) of succinic anhydride. The resulting solution was stirred for 1.5 h and then cooled to 0 °C. After cautious addition of 4 mL of concentrated HCl, the solution was extracted with 16 25-mL portions of $CHCl_3$. The combined organic layers were dried with Na_2SO_4 and evaporated to give 4.96 g (86%) of the mono-*N,N*-dimethylamide of succinic acid as a white crystalline solid: ^{1}H NMR ($CDCl_3$) δ 2.68 (m, 4 H, CH_2CH_2), 2.97 (s, 3 H, CH_3), 3.05 (s, 3 H, CH_3). This material was carried on without further purification.

Activation of this dimethylamide acid as the *N*-hydroxybenzotriazole ester, through the intermediacy of DCC, and in situ trapping with methylamine were carried out as described above. The crude product was chromatographed on SiO_2 eluting with 5% MeOH in CH_2Cl_2 to give the desired diamide as a hygroscopic off-white solid in 90% yield: mp 69–70

(32) For a recent review of ring closure effects in systems involving formation of a full covalent bond, see: Mandolini, L. *Adv. Phys. Org. Chem.* **1986**, *22*, 1.

(33) For leading references, see: (a) Mackay, D. H. J.; Cross, A. T.; Hagler, A. T. In *Prediction of Protein Structure and the Principles of Protein Conformation*; Fasman, G. D., Ed.; Plenum Press: New York, 1989; pp 317–358. (b) Lii, J. H.; Gallion, S.; Bender, C.; Wikstrom, H.; Allinger, N. L.; Flurchick, K. M.; Teeter, M. M. *J. Comput. Chem.* **1989**, *10*, 503. (c) Weiner, S. J.; Kollman, P. A.; Nguyen, D. T.; Case, D. A. *J. Comput. Chem.* **1986**, *7*, 230. (d) Tirado-Rives, J.; Jorgensen, W. L. *J. Am. Chem. Soc.* **1990**, *112*, 2773. (e) Brooks, B. R.; Bruccoleri, R. E.; Olafson, B. D.; States, D. J.; Swaminathan, S.; Karplus, M. *J. Comput. Chem.* **1983**, *4*, 187.

°C (after several days in a drying pistol); ^{1}H NMR ($CDCl_3$) δ 2.51 (m, 2 H, CH_2), 2.67 (m, 2 H, CH_2), 2.78 (d, J = 4.8 Hz, 3 H, $NHCH_3$), 2.95 (s, 3 H, CH_3), 3.03 (s, 3 H, CH_3), 6.31 (broad, 1 H, NH); IR (1 mM in CH_2Cl_2) 3457 (NH), 3350 (broad, NH), 1670 (C=O), 1642 (C=O) cm^{-1}. EI MS m/e: 158.1067. Calcd for $C_7H_{14}N_2O_2$: 158.1055.

***N,N,N'*-Trimethylpentanediamide (3)** was prepared analogously, starting from glutaric anhydride. The intermediate dimethylamide acid was isolated without purification in 83% yield as a white crystalline solid: ^{1}H NMR ($CDCl_3$) δ 1.95 (m, 2 H, CH_2), 2.44 (m, 4 H, 2×CH_2), 2.96 (s, 3 H, CH_3), 3.04 (s, 3 H, CH_3). After activation and reaction with methylamine, diamide **3** was isolated by SiO_2 chromatography as an off-white hygroscopic solid in 81% yield: mp 59–60 °C (after several days in a drying pistol); ^{1}H NMR ($CDCl_3$) δ 1.95 (m, 2 H, CH_2), 2.28 (t, J = 7.0 Hz, 2 H, CH_2), 2.41 (t, J = 7.0 Hz, 2 H, CH_2), 2.80 (d, J = 4.8 Hz, 3 H, $NHCH_3$), 2.95 (s, 3 H, NCH_3), 3.02 (s, 3 H, NCH_3), 6.13 (broad, 1 H, NH); IR (1 mM in CH_2Cl_2) 3458 (NH), 3320 (broad, NH), 1671 (C=O), 1640 (C=O) cm^{-1}. EI MS m/e: 172.1203. Calcd for $C_8H_{16}N_2O_2$: 172.1212.

***N,N,N'*-Trimethylhexanediamide (4).** A mixture of 7.3 g of adipic acid (50 mmol) and 10 mL of acetyl chloride (140 mmol) was refluxed for 1 h. Excess acetyl chloride was removed by distillation under reduced pressure (aspirator), and the resulting residue was further dried on a vacuum line. This polymeric mass was manually broken up and mixed with 25 mL of 40 wt % aqueous dimethylamine (200 mmol). The mixture was allowed to stir for 18 h, during which time the suspended solid slowly dissipated. The resulting solution was cooled to 0 °C and acidified by cautious addition of concentrated HCl to pH <1. A large amount of white precipitate formed during this process; this material was isolated by suction filtration and proved to be adipic acid. The filtrate was washed with 10 50-mL portions of $CHCl_3$. Combined organic layers were dried over Na_2SO_4 and evaporated to give 5.9 g of viscous colorless liquid. The ^{1}H NMR spectrum of this material was consistent with a mixture of the mono- and bis(*N,N*-dimethylamide)s of adipic acid. A portion of this material (1.8 g) was mixed with azeotropically dried *N*-hydroxybenzotriazole (2.0 g before drying, ca. 12 mmol) and 2.5 g of DCC (12 mmol) in 30 mL of THF under N_2. The reaction solution was initially clear, but a white precipitate quickly developed. After 2.5 h, the slurry was filtered through a glass frit under positive N_2 pressure. The filtrate was cooled to 0 °C (under positive N_2 pressure), and CH_3NH_2 was bubbled through for 10 min. The reaction mixture was allowed to warm to room temperature and stir for 17 h. The crude product was chromatographed on a SiO_2 column eluting with 5% MeOH in CH_2Cl_2. The desired diamide was isolated as a hygroscopic off-white solid (0.49 g, 17% from adipic acid): mp 58–59 °C (after several days in a drying pistol) (lit.[34] 54–56 °C); ^{1}H NMR ($CDCl_3$) δ 1.66 (m, 4 H, CH_2CH_2), 2.24 (m, 2 H, CH_2), 2.34 (m, 2 H, CH_2), 2.81 (d, J = 4.8 Hz, 3 H, $NHCH_3$) 2.95 (s, 3 H, CH_3), 3.00 (s, 3 H, CH_3), 6.23 (broad, 1 H, NH); IR (1 mM in CH_2Cl_2) 3459 (NH), 3320 (broad, NH), 1671 (C=O), 1638 (C=O) cm^{-1}. EI MS m/e: 186.1372. Calcd for $C_9H_{18}N_2O_2$: 186.1368. Eluting just before triamide **4** was *N,N,N',N'*-tetramethylhexanediamide, an off-white solid (0.22 g, 7% from adipic acid): mp 81.5–82.5 °C (lit.[35] 85 °C); ^{1}H NMR ($CDCl_3$) δ 1.68 (m, 4 H, CH_2), 2.35 (m, 4 H, CH_2), 2.94 (s, 6 H, CH_3), 3.01 (s, 6 H, CH_3); IR (10 mM in CH_2Cl_2) 1640 (C=O) cm^{-1}. EI MS m/e: 200.1513. Calcd for $C_{10}H_{20}N_2O_2$: 200.1525.

***N,N,N'*-Trimethylheptanediamide (5)** was prepared from pimelic acid by an analogous multistep procedure. Diamide **5** was isolated after chromatography on SiO_2 as a hygroscopic off-white solid in 25% overall yield: mp 62–63 °C (after several days in a drying pistol); ^{1}H NMR ($CDCl_3$) δ 1.38 (m, 2 H, CH_2), 1.66 (m, 4 H, CH_2), 2.20 (m, 2 H, CH_2), 2.32 (m, 2 H, CH_2), 2.80 (d, J = 4.8 Hz, 3 H, $NHCH_3$), 2.94 (s, 3 H, CH_3), 3.00 (s, 3 H, CH_3), 5.73 (broad, 1 H, NH); IR (1 mM in CH_2Cl_2) 3459 (NH), 3340 (broad, NH), 1671 (C=O), 1639 (C=O) cm^{-1}. EI MS m/e: 200.1544. Calcd for $C_{10}H_{20}N_2O_2$: 200.1525. Eluting just before triamide **5** from the column was *N,N,N',N'*-tetramethylheptanediamide, a yellow-tinted oil (7% from pimelic acid): ^{1}H NMR ($CDCl_3$) δ 1.42 (m, 2 H, CH_2), 1.67 (m, 4 H, CH_2), 2.30 (m, 4 H, CH_2), 2.94 (s, 6 H, CH_3), 3.00 (s, 6 H, CH_3); IR (10 mM in CH_2Cl_2) 1639 (C=O) cm^{-1}. EI MS m/e 214.1679. Calcd for $C_{11}H_{22}N_2O_2$: 200.1681.

***N,N,N'*-Trimethyloctanediamide (6)** was prepared from suberic acid by an analogous multistep procedure. Diamide **6** was isolated after chromatography on SiO_2 as a hygroscopic off-white solid in 27% overall yield: mp 64.5–66 °C (after several days in a drying pistol); ^{1}H NMR ($CDCl_3$) δ 1.35 (m, 4 H, CH_2), 1.64 (m, 4 H, CH_2), 2.17 (m, 2 H, CH_2), 2.31 (m, 2 H, CH_2), 2.80 (d, J = 4.8 Hz, 3 H, $NHCH_3$), 2.94 (s, 3 H, CH_3), 3.00 (s, 3 H, CH_3), 5.66 (broad, 1 H, NH); IR (1 mM in CH_2Cl_2) 3460 (NH), 1671 (C=O), 1639 (C=O) cm^{-1}. EI MS m/e: 214.1684. Calcd for $C_{11}H_{22}N_2O_2$: 214.1681. Eluting just before triamide **6** from the column was *N,N,N',N'*-tetramethyloctanediamide, an off-white solid (5% from suberic acid): mp 85.5–86.5 °C; ^{1}H NMR ($CDCl_3$) δ 1.37 (m, 4 H, CH_2), 1.65 (m, 4 H, CH_2), 2.31 (m, 4 H, CH_2), 2.94 (s, 6 H, CH_3), 3.00 (s, 6 H, CH_3); IR (10 mM in CH_2Cl_2) 1639 cm^{-1}. EI MS m/e: 228.1823. Calcd for $C_{12}H_{24}N_2O_2$: 228.1838.

***N,N*-Dimethylmalonamide Methyl Ester (7).** A mixture of 5.8 g of Meldrum's acid (0.04 mmol), 8 mL of H_2O, and 25 mL of 40 wt % aqueous methylamine was stirred for 52 hr. The solution was then cooled to 0 °C and acidified by cautious addition of 17 mL of concentrated HCl. This solution was concentrated on a vacuum rotary evaporator. The residue was taken up in 70 mL of H_2O, a solution of 6 mL of concentrated H_2SO_4 in 50 mL of MeOH was added, and the solution was allowed to stand for 84 h. Another 100 mL of H_2O was added, and the solution was extracted with eight 50-mL portions of CH_2Cl_2. The combined organic layers were dried over Na_2SO_4 and evaporated to a brown oil. This material was purified by SiO_2 column chromatography, eluting with 2.5% MeOH in $CHCl_3$, to give the desired amide ester as a colorless liquid in 29% yield: ^{1}H NMR ($CDCl_3$) δ 2.85 (d, J = 4.9 Hz, 3 H, $NHCH_3$), 3.33 (s, 2 H, CH_2), 3.75 (s, 3 H, OCH_3), 7.12 (broad, 1 H, NH); IR (1 mM in CH_2Cl_2) 3454 (NH), 3390 (NH), 1727 (ester C=O), 1679 (amide C=O) cm^{-1}. EI MS m/e: 131.0580. Calcd for $C_5H_9NO_3$: 131.0582.

***N,N*-Dimethylsuccinamide Methyl Ester (8).** A mixture of 8 mL of 40 wt % aqueous methylamine and 8 mL of H_2O was cooled to 0 °C, and then 4.0 g (0.04 mol) of solid succinic anhydride was added in small portions. The resulting solution was allowed to warm to room temperature 1 h and then recooled to 0 °C. The cold solution was acidified to pH ≤1 by cautious addition of 8 mL of concentrated HCl. This solution was concentrated to dryness on a vacuum rotary evaporator, and the residue was vacuum desiccated for several days. The resulting sticky white material was Soxhlet-extracted with CH_2Cl_2 for 2 days. The organic solution was then evaporated to give 4.6 g of a white solid, the ^{1}H NMR spectrum of which indicated it to be predominantly the desired monomethylamide acid. This material was carried on immediately: 0.65 g was dissolved in 10 mL of 10:1 MeOH concentrated H_2SO_4. After 47 h, this solution was diluted with 50 mL of H_2O and extracted with six 25-mL portions of CH_2Cl_2. The combined organic layers were dried over Na_2SO_4 and evaporated to a yellow oil that was purified by SiO_2 column chromatography, eluting with 2.5% MeOH in $CHCl_3$, to give 0.36 g (50% overall) of the desired amide ester as a white crystalline solid: mp 54–55 °C; ^{1}H NMR ($CDCl_3$) δ 2.47 (m, 2 H, CH_2), 2.68 (m, 2 H, CH_2), 2.81 (d, J = 4.8 Hz, 3 H, $NHCH_3$), 3.69 (s, 3 H, OCH_3), 5.77 (broad, 1 H, NH); IR (1 mM in CH_2Cl_2) 3457 (NH), 1735 (ester C=O), 1678 (amide C=O) cm^{-1}. EI MS m/e: 145.0734. Calcd for $C_6H_{11}NO_3$: 145.0739.

***N,N*-Dimethylglutaramide methyl ester (9)** was prepared analogously, in 37% overall yield from glutaric anhydride; the desired product proved to be a colorless low-melting solid: ^{1}H NMR ($CDCl_3$) δ 1.97 (m, 2 H, CH_2), 2.24 (m, 2 H, CH_2), 2.39 (m, 2 H, CH_2), 2.81 (d, J = 4.8 Hz, 3 H, $NHCH_3$), 3.68 (s, 3 H, OCH_3), 5.60 (broad, 1 H, NH); IR (1 mM in CH_2Cl_2) 3458 (NH), 1733 (ester C=O), 1674 (amide C=O) cm^{-1}. EI MS m/e: 159.0905. Calcd for $C_6H_{11}NO_3$: 159.0895.

***N,N*-Dimethyladipamide Methyl Ester (10).** A mixture of 7.3 g of adipic acid (50 mmol) and 10 mL of acetyl chloride (140 mmol) was refluxed for 1 h. Excess acetyl chloride was removed by distillation under reduced pressure (aspirator), and the resulting residue was further dried on a vacuum line. This polymeric mass was manually broken up and mixed with 25 mL of 40 wt % aqueous methylamine (200 mmol). The mixture was allowed to stir for 1 h at 0 °C, during which time the suspended solid slowly dissipated, and then for 10 h at room temperature. The resulting solution was cooled to 0 °C and acidified by cautious addition of 20 mL of concentrated HCl (to pH <1). A large amount of white precipitate (adipic acid) formed during this process; this material was removed by suction filtration. The filtrate was concentrated to a viscous residue on a vacuum rotary evaporator and then further desiccated in vacuo. The material was then taken up in 50 mL of H_2O and continuously extracted with Et_2O for 2.5 days. The ether layer was evaporated to yield 5.09 g of white solid, which ^{1}H NMR indicated to contain the desired monomethylamide acid and other components. This material was immediately carried on: 1.6 g was dissolved in 22 mL of 10:1 MeOH/concentrated H_2SO_4. After 48 h, the solution was diluted with 100 mL of H_2O and extracted with six 50-mL portions of CH_2Cl_2. The combined organic layers were dried over Na_2SO_4 and evaporated to an oil that was subjected to SiO_2 column chromatography. The desired product was eluted with 5% MeOH in $CHCl_3$ as a colorless oil that slowly crystallized (0.92 g, 53% from adipic acid): mp 47–48 °C; ^{1}H NMR ($CDCl_3$) δ 1.66 (m, 4 H, CH_2), 2.20 (m, 2 H, CH_2), 2.34 (m, 2 H, CH_2), 2.80 (d, J = 4.8 Hz, 3 H, $NHCH_3$), 3.67 (s, 3 H, OCH_3), 5.78 (broad,

(34) Carey, F. M.; Furst, C. I.; Lewis, J. J.; Stenlake, J. B. *J. Pharm. Pharmacol. Suppl.* **1964**, *16*, 89T-103T.

(35) Prelog, V. *Collect. Czech. Chem. Commun.* **1930**, *2*, 712.

1 H, NH); IR (1 mM in CH_2Cl_2) 3459 (NH), 1733 (ester C=O), 1673 (amide C=O) cm^{-1}. EI MS *m/e*: 173.1045. Calcd for $C_6H_{11}NO_3$: 173.1052.

Variable-Temperature NMR Experiments. All amides used for preparation of CD_2Cl_2 solutions for variable-temperature ^1H NMR experiments were vacuum-desiccated in a heated drying pistol in the presence of P_2O_5 for several days before sample preparation. The CD_2Cl_2 was stirred with CaH_2 overnight and then distilled onto activated 4-Å molecular sieves under N_2 immediately before use. Syringes and NMR tubes were dried on a vacuum line at room temperature overnight. The samples were prepared in a glovebag (N_2) by dissolving a 5-20-mg portion of the dried amide in sufficient CD_2Cl_2 to make a 100 mM solution and then performing two serial 1:9 dilutions with CD_2Cl_2. The resulting 1 mM solution was placed in an NMR tube, freeze-pump-thaw degassed, and sealed under vacuum. Even with these precautions, the resulting samples typically contained 5-10 mM H_2O. CD_3CN NMR samples (10 mM) were prepared without special precautions. For samples prepared in 9:1 CCl_4/C_6D_6 (1 mM), the CCl_4 was dried by passage over a column of alumina.

Variable-temperature NMR measurements were performed on a Bruker AM-500 spectrometer. A microprogram was used to change temperature in fixed increments automatically, wait 15 min for temperature to stabilize, refine the *Z* and Z^2 shims, and then obtain a 128-scan spectrum. In one run, measurements were made in the range 193-273 or 253-303 K for CD_2Cl_2 or 253-323 K for CD_3CN. In these experiments, the first measurement was made at the lowest temperature, and then the temperature was increased in 10 K increments. At the top of the range, the temperature was dropped by 5 K and then by additional 10 K increments. For measurements in CD_2Cl_2, all chemical shifts were referenced to the signal for residual $CHDCl_2$, which was assumed to be 5.320 ppm *at all temperatures*. For measurements in CD_3CN, chemical shifts were referenced to residual CHD_2CN, at 1.950 ppm. From one run to another, amide proton chemical shift measurements at a given temperature were generally reproducible to within 0.05 ppm (with the same sample or an independently prepared sample). For thermodynamic analyses, nominal probe temperatures, read directly from the spectrometer console, were converted to actual temperatures by means of a calibration curve constructed with a chemical shift thermometer (0.03% concentrated HCl in MeOH).[36]

Variable-Temperature IR Experiments. Amides used for preparation of IR samples were vacuum-desiccated as described for NMR samples. CH_2Cl_2 solutions were prepared in a glovebag (N_2) by dissolving several milligrams of amide in solvent that had been distilled from CaH_2 under N_2 to yield 10-100 mM samples and performing serial dilutions to 1 mM. Acetonitrile samples (10 mM) were prepared from solvent stored over 3-Å molecular sieves. Baseline corrections were applied to obtain the spectra reproduced in Figures 1 and 2, but baseline corrections were *not* applied when quantitative analysis of the data was performed.

IR measurements were performed on a Nicolet 740 FT-IR instrument equipped with a TGS detector. A Specac variable-temperature cell P/N 21.500 equipped with CaF_2 windows and having a path length of 1.0 mm was used for variable-temperature experiments. Temperatures were maintained with various ice, dry ice, or liquid N_2 slush baths and were monitored with a platinum resistance thermometer attached directly to the cell. The cell temperature was allowed to stabilize for at least 20 min before measurements were obtained, and the cell temperature varied less than 1 °C during data acquisition. Spectra of 128 scans were obtained with 2-cm^{-1} resolution. Solvent subtraction was carried out by using reference spectra obtained at approximately the same temperatures as the sample spectra.

Acknowledgment. We are grateful to the Searle Scholars Program and the Petroleum Research Fund, administered by the American Chemical Society, for support of this research. S.H.G. thanks the American Cancer Society for a Junior Faculty Research Award. We are indebted to Professor R. J. McMahon for helpful comments and advice.

(36) Van Geet, A. L. *Anal. Chem.* **1970**, *42*, 679.

Quasi-Equilibration of $N(a) + {}^1/_2H_2 \rightleftharpoons NH$ Established on c(2×2)-N of the Pd(100), Rh(100), and Pt-Rh(100) Surfaces during Hydrogenation of c(2×2)-N

Taro Yamada and Ken-ichi Tanaka*

Contribution from the Institute for Solid State Physics, The University of Tokyo, 7-22-1 Roppongi, Minato-ku, Tokyo 106, Japan. *Received June 1, 1990. Revised Manuscript Received October 11, 1990*

Abstract: Pd, Rh, and Pt are inert for the dissociative adsorption of N_2 and make no bulk nitrides, but we can prepare a nitrogen overlayer with the c(2×2) structure on Pd(100), Rh(100), and Pt-Rh(100) surfaces by the reaction of $NO + H_2 \rightarrow N(a) + H_2O$. When the nitrogen overlayer denoted by c(2×2)-N was exposed to 10^{-6}-10^{-8} Torr of H_2 at around 400 K, a prominent energy loss peak appeared at 3200-3240 cm^{-1}. Pressure dependence of the in situ energy loss spectrum proved that a quasi-equilibration of $N(a) + {}^1/_2H_2 \rightleftharpoons NH$ is established on the Rh(100) surface at 400 K, but the c(2×2) LEED pattern changes little by being exposed to H_2. These results indicate that the NH species is prominently formed at the surroundings of the c(2×2)-N islands when the c(2×2)-N surface is exposed to H_2. The isotope effect on this quasi-equilibration was shown to be very small on the Rh(100) surface as well as on the Pd(100) and Pt-Rh(100) surfaces, which is in remarkable contrast to the large inverse isotope effect reported on the ammonia synthesis reaction.

Introduction

Pd, Rh, and Pt are inert for dissociative adsorption of N_2[1] so that they have no catalytic activity for ammonia synthesis reaction. Furthermore, these metals make no bulk nitrides.[2] On the other hand, these metals catalyze the reaction of NO_x with H_2 or CO. Provided that the NO molecule undergoes the following reactions on the metals surfaces, nitrogen intermediates should be formed on these metal surfaces during the reaction. Provided that re-

* To whom correspondence should be addressed.

(1) Cf: Hayward, D. O.; Trapnell, B. M. W. *Chemisorption*; Butterworths: London, 1964.

(2) Cf: Wells, A. F. *Structural Inorganic Chemistry*, 5th ed.; Clarendon Press: Oxford, U.K., 1984; p 207.

0002-7863/91/1513-1173$02.50/0